

Self-Healing Heterometallic Supramolecular Polymers Constructed by Hierarchical Assembly of Triply Orthogonal Interactions with Tunable Photophysical Properties

Qian Zhang, Danting Tang, Jinjin Zhang, Ruidong Ni, Luonan Xu, Tian He,
Xiongjie Lin, Xiaopeng Li, huayu qiu, Shouchun Yin, and Peter J. Stang

J. Am. Chem. Soc., **Just Accepted Manuscript** • DOI: 10.1021/jacs.9b09671 • Publication Date (Web): 16 Oct 2019

Downloaded from pubs.acs.org on October 20, 2019

Just Accepted

“Just Accepted” manuscripts have been peer-reviewed and accepted for publication. They are posted online prior to technical editing, formatting for publication and author proofing. The American Chemical Society provides “Just Accepted” as a service to the research community to expedite the dissemination of scientific material as soon as possible after acceptance. “Just Accepted” manuscripts appear in full in PDF format accompanied by an HTML abstract. “Just Accepted” manuscripts have been fully peer reviewed, but should not be considered the official version of record. They are citable by the Digital Object Identifier (DOI®). “Just Accepted” is an optional service offered to authors. Therefore, the “Just Accepted” Web site may not include all articles that will be published in the journal. After a manuscript is technically edited and formatted, it will be removed from the “Just Accepted” Web site and published as an ASAP article. Note that technical editing may introduce minor changes to the manuscript text and/or graphics which could affect content, and all legal disclaimers and ethical guidelines that apply to the journal pertain. ACS cannot be held responsible for errors or consequences arising from the use of information contained in these “Just Accepted” manuscripts.

1
2
3
4 **Self-Healing Heterometallic Supramolecular Polymers Constructed**
5
6 **by Hierarchical Assembly of Triply Orthogonal Interactions with**
7
8 **Tunable Photophysical Properties**
9

10
11 Qian Zhang,^{†,‡,#} Danting Tang,^{†,#} Jinjin Zhang,[†] Ruidong Ni,[§] Luonan Xu,[†] Tian He,[†]
12 Xiongjie Lin,[†] Xiaopeng Li,[§] Huayu Qiu,[†] Shouchun Yin,^{*,†} Peter J. Stang^{*,‡}
13
14

15 [†]College of Materials, Chemistry and Chemical Engineering, Hangzhou Normal
16 University, Hangzhou 310036, P. R. China.
17

18 [‡]Department of Chemistry, University of Utah, 315 South 1400 East, Room 2020, Salt
19 Lake City, Utah 84112, United States.
20

21 [§]Department of Chemistry, University of South Florida, 4202 East Fowler Avenue,
22 Tampa, Florida 33620, United States.
23
24
25
26
27

28 **ABSTRACT**
29

30 Here we present a method for the building of new bicyclic heterometallic cross-linked
31 supramolecular polymers by hierarchical unification of three types of orthogonal
32 noncovalent interactions, including platinum(II)-pyridine coordination-driven
33 self-assembly, zinc-terpyridine complex and host-guest interactions. The
34 platinum-pyridine coordination provides the primary driving force to form discrete
35 rhomboidal metallacycles. The assembly doesn't interfere with the zinc-terpyridine
36 complexes, which link the discrete metallacycles into linear supramolecular polymers,
37 and the conjugation length is extended upon the formation of the zinc-terpyridine
38 complexes, which redshifts the absorption and emission spectra. Finally, host-guest
39 interactions via bis-ammonium salt binding to the benzo-21-crown-7 (B21C7) groups
40 on the platinum acceptors afford the cross-linked supramolecular polymers. By
41 continuous increase of the concentration of the supramolecular polymer to a relatively
42 high level, supramolecular polymer gel is obtained, which exhibits self-healing
43 properties and reversible gel-sol transitions stimulated by various external stimuli,
44 including temperature, K⁺ and cyclen. Moreover, the photophysical properties of the
45
46
47
48
49
50
51
52
53
54
55
56
57
58
59
60

1
2
3 supramolecular polymers could be effectively tuned by varying the substituents of the
4 precursor ligands.
5
6

7 8 **INTRODUCTION**

9
10 Supramolecular polymers,¹ i.e. polymeric arrays of monomer units that are
11 assembled by reversible and highly directional noncovalent bonds, have gained
12 remarkable attention due to the combination of the conventional polymeric properties
13 and the fascinating features like stimuli-responsive and self-healing capabilities.²⁻⁹
14 The dynamic properties of these materials deriving from the reversible noncovalent
15 bonds make supramolecular polymers attractive for various applications, such as drug
16 delivery, biosensors, tissue engineering, optical devices, actuators and coatings and
17 textiles.¹⁰⁻¹⁵
18

19 Among the miscellaneous noncovalent interactions, such as metal-ligand
20 coordination, host-guest interactions, H-bonding, π - π stacking, van der Waals forces,
21 hydrophobic forces, etc, metal-ligand coordination is of particular interest due to its
22 high directionality and strong strength approaching that of covalent bonds.¹⁶⁻¹⁸
23 Metal-ligand coordination has been demonstrated to be an efficient strategy for
24 preparing supramolecular polymers since it allows the construction of well-defined
25 supramolecular architectures and endows the resulting polymers with higher stability
26 in comparison with other noncovalent interactions.¹⁹⁻²¹ Meanwhile,
27 coordination-driven polymers could combine the properties of organic polymers with
28 the photophysical, magnetic, electronic, and catalytic potential of metals. The
29 chemistry of metal-terpyridine complexes is a particularly powerful tool for the
30 building of supramolecular architectures and polymers, since terpyridine moieties are
31 capable of forming strong, directed and reversible complexes with a variety of metal
32 ions due to $d\pi$ - $p\pi^*$ back-bonding of the metal to pyridine rings and the chelate
33 effect.²²⁻²⁸ For example, Schubert and coworkers reported a linear water-soluble
34 metallo-supramolecular polymer based on iron(II)/terpyridine complexes, which
35 showed high thermal stability and reversible properties.²²
36
37
38
39
40
41
42
43
44
45
46
47
48
49
50
51
52
53
54
55

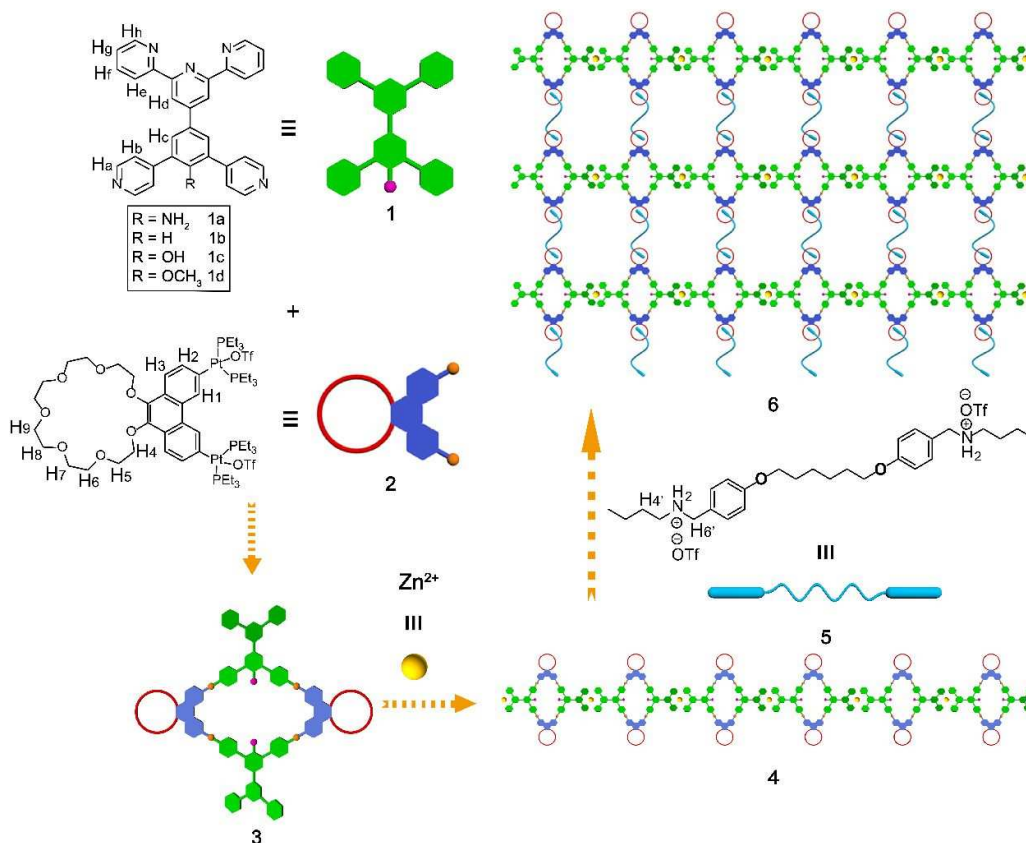
56 Supramolecular polygons and polyhedrons with well-defined sizes, shapes and
57

1
2
3 geometries could be readily constructed via the metal-ligand coordination-driven
4 self-assembly.²⁹⁻⁴² Using a selective and reasonable choice of precursors, Stang,²⁹
5 Fujita,³⁰ Raymond,³³ Nitschke,²⁸ and others have designed and synthesized a library
6 of elegant two-dimensional metallacycles and three-dimensional metallacages, which
7 are increasingly of interest in various applications such as encapsulation, catalysis,
8 chemosensing, and light harvesting. Because of the well-defined structures of
9 metallacycles, multiple functional moieties can be easily covalently appended either
10 on the periphery or at the vertices of predesigned metallacyclic skeletons, which
11 afford the chance to introduce other types of noncovalent interactions for orthogonal
12 hierarchical self-assembly.⁴³⁻⁴⁶ Via orthogonal combination of metal-ligand
13 coordination-driven self-assembly with other different noncovalent interactions,
14 multifunctional metallacycle- or metallacage-cored supramolecular polymers could be
15 readily accessed.^{16,45,47} For example, Stang and coworkers reported several functional
16 supramolecular polymers with fascinating properties by the unification of
17 platinum(II)-ligand coordination-driven self-assembly with hydrogen bonding or
18 crown ether-based host-guest interactions.^{43,48-50} However, it is still very challenging
19 to prepare the well-controlled hierarchical self-assembly of organometallic materials
20 with higher-order structures, especially the stimuli-responsive smart soft materials.
21 Superstructures assembled via three or more types of orthogonal noncovalent
22 interactions that do not interfere with one another, are rarely reported.⁵¹ Up to now,
23 usually only one type of metal-ligand binding motif was incorporated in those
24 structures. It is intriguing to functionalize the architectures with secondary metal sites,
25 which could furnish the materials with more novel functionalities, such as
26 electrochemical, photophysical or magnetic properties.⁵²

27
28
29
30
31
32
33
34
35
36
37
38
39
40
41
42
43
44
45
46
47
48
49
50
51
52
53
54
55
56
57
58
59
60

Herein, in addition to platinum(II)←pyridine coordination motif, we introduced a second coordination motif, the terpyridine-zinc(II) complex to the backbone of the supramolecular polymers. To this end, a heterometallic cross-linked supramolecular polymer was constructed by the hierarchical unification of three types of noncovalent interactions, platinum(II)-ligand coordination-driven self-assembly, zinc(II)-terpyridine complex and host-guest interactions. As shown in Scheme 1,

1
2
3 ditopic ligands with one end terminating with a terpyridyl moiety and the other
4 terminating with a 120° dipyridyl fragment, bearing different substituents were
5 synthesized, wherein platinum(II) could bind to the 120° dipyridyl moiety to form
6 rhomboidal metallacycles, and then the terminal terpyridines can coordinate with
7 Zn(II) into linear supramolecular polymers. To the best of our knowledge, this is the
8 first time to develop linear supramolecular polymers with heterometallic bicyclic
9 metallacycles in the backbone. The conjugation length was extended after the
10 zinc-terpyridine complexes formed, which redshifted the absorption and emission
11 spectra. Then, a supramolecular polymer network gel was obtained by adding the
12 cross-linker, bis-ammonium salt, to the solution of the linear supramolecular polymer.
13 The cross-linked supramolecular polymer was found to form supramolecular gels at
14 high concentrations in appropriate solvents, demonstrating that multi-functional smart
15 soft materials could be accessed using the strategy developed here. Furthermore, the
16 photophysical properties of the metallacycles and cross-linked supramolecular
17 polymers could be effectively tuned via changing the substituents on the precursor
18 ligands.
19
20
21
22
23
24
25
26
27
28
29
30
31
32
33
34
35
36
37
38
39
40
41
42
43
44
45
46
47
48
49
50
51
52
53
54
55
56
57
58
59
60



Scheme 1 Cartoon representation of the formation of rhomboidal metallacycles, a linear supramolecular polymer and a cross-linked 3D supramolecular polymeric network from metallacycles, Zn^{2+} and bis-ammonium salts.

RESULTS AND DISCUSSION

The rhomboidal metallacycles were obtained by stirring a mixture of the 120° dipyrindyl heteroditopic ligand **1a-1d** and an equimolar amount of 60° organo-diplatinum (II) acceptor **2** in $\text{DMSO-}d_6$ at 65 °C for 12 h. These rhomboids were pendent with benzo-21-crown-7 (B21C7) at their acute vertices and terpyridine moieties at their obtuse vertices, respectively. The detailed synthetic procedures for the ligands and metallacycles are given in the Supporting Information (SI). These chemical structures of the ligands and the formation of discrete and highly symmetric species were confirmed by multinuclear (^1H and ^{31}P) NMR analyses (Figure S1-S38). Here, we use **3a** as a representative example. In the ^1H NMR spectrum of metallacycle **3a** (Figure 1a-1c), the protons of the pyridyl groups exhibited downfield

1
2
3 shifts compared with those of the free ligand **1a** due to the loss of electron density
4 upon coordination of the pyridine N atom with the platinum (II) centers. Besides, a
5 splitting of the H_a and H_b peaks was observed (H_a from 8.68 to 9.00 and 8.90 ppm; H_b
6 from 7.55 to 8.45 and 8.33 ppm). The assignment and correlation of the protons on
7 the metallacycle was validated by ¹H-¹H homonuclear correlation spectroscopy
8 (COSY) NMR experiments (Figure S29). The ³¹P NMR spectrum of rhomboid **3a**
9 showed a sharp singlet at 14.10 ppm with concomitant ¹⁹⁵Pt satellites ($J_{\text{Pt-P}} = 2678.1$
10 Hz), in accordance with a single phosphorous environment. This peak was upfield
11 shifted by 6.02 ppm relative to that of the platinum(II) acceptor (Figure 1d and 1e).
12 Electro spray ionization time-of-flight mass spectrometry (ESI-TOF-MS) further
13 demonstrated the stoichiometry of the formation of rhomboids (Figure 1f). An
14 isotopically resolved peak corresponding to the intact and discrete [2 + 2] assembly
15 **3a** with the loss of three trifluoromethanesulfonate (OTf) counterions was observed
16 at m/z 1247.20 [M - 3OTf]³⁺, which provided convincing evidence for the existence
17 of the rhomboidal metallacycle as the only supramolecular species. Likewise, all other
18 metallacycles gave the similar results as shown in the SI.
19
20
21
22
23
24
25
26
27
28
29
30
31
32
33
34
35
36
37
38
39
40
41
42
43
44
45
46
47
48
49
50
51
52
53
54
55
56
57
58
59
60

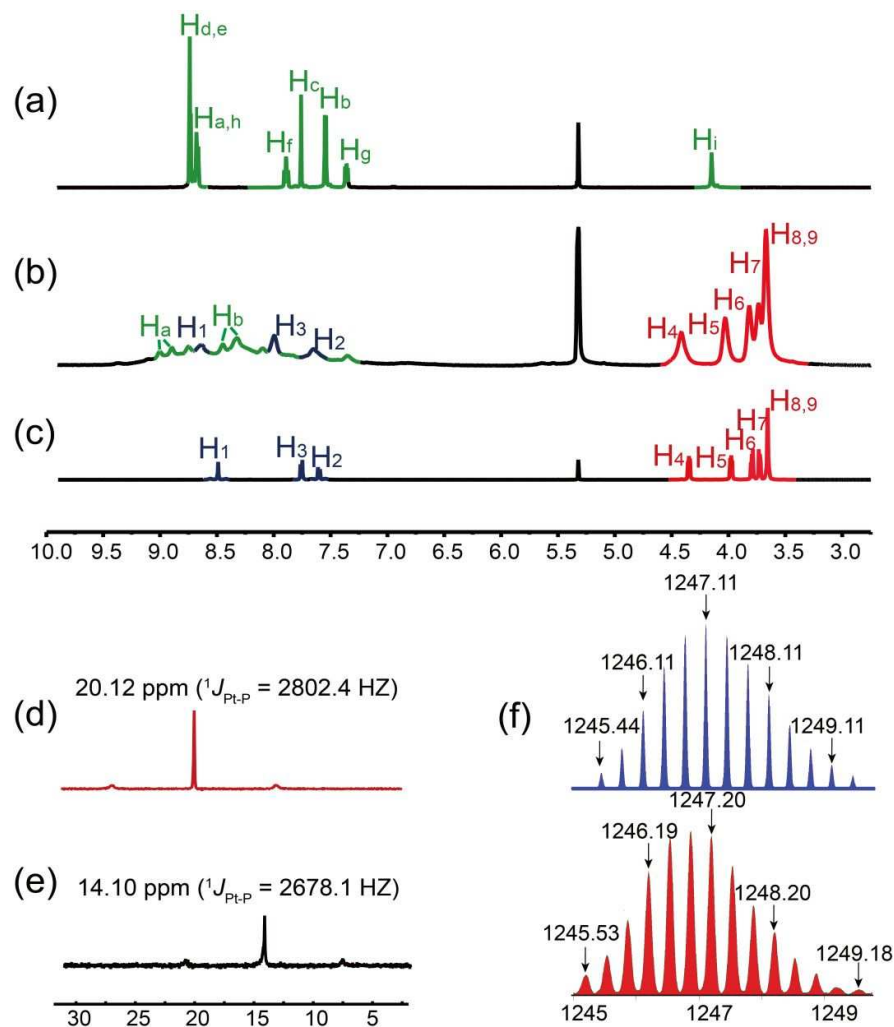


Figure 1. Partial (a-c) ^1H and (d, e) ^{31}P NMR spectra [$\text{CD}_3\text{CN}/\text{CD}_2\text{Cl}_2$ (1:1, v/v), 295 K] of (a) $\mathbf{1a}$, (b, e) $\mathbf{3a}$, (c, d) acceptor $\mathbf{2}$. (f) Experimental (red) and calculated (blue) ESI-TOF-MS spectra of rhomboidal metallacycle $\mathbf{3a}$ [$\text{M} - 3\text{OTf}$] $^{3+}$.

Subsequently, the linear supramolecular polymer $\mathbf{4a}$ was formed by the coordination between $\text{Zn}(\text{OTf})_2$ and terpyridine moieties, which was investigated by UV-Vis spectroscopy. A UV-Vis titration was performed by stepwise adding a solution of $\text{Zn}(\text{OTf})_2$ to a $\text{CH}_2\text{Cl}_2/\text{CH}_3\text{CN}$ solution of $\mathbf{3a}$ (Figure 2a). The absorbance of the band at 392 nm corresponding to the characteristic of zinc-terpyridine complex gradually increased, and a distinct isosbestic point at 340 nm appeared, indicating the successful formation of the zinc-terpyridine complexes. As shown in Figure 2b, the absorbance at 392 nm almost remained constant after the addition of one equivalent of

Zn²⁺, indicating a 1:1 ligand-to-metal stoichiometry, which is consistent with our assumption as illustrated in Scheme 1. The binding constant K_a of Zn²⁺ and **1a** determined by UV-Vis titration is calculated to be 38000 M⁻¹ (Figure S39). The linear supramolecular polymerization behavior of the monomers was then studied by various methods, including the concentration-dependent ¹H NMR, diffusion-ordered ¹H NMR spectroscopy (DOSY) and dynamic light scattering (DLS) measurements. As shown in Figure S40, by increasing the monomer concentration from 1 to 60 mM, the signals of protons H_g and H_h upfield and downfield shifted, respectively, and all the peaks of the protons became broad. As the monomer concentration increased from 5 to 60 mM, the weight-average diffusion coefficient (D) considerably decreased from 4.2×10^{-9} to 7.2×10^{-10} m² s⁻¹, indicating the formation of high-molecular-weight-supramolecular polymers (Figure S41a). The DLS results showed that the average hydrodynamic diameters (D_h) of the assemblies at low (2.0 mM) and high (60.0 mM) concentration were determined to be 93 and 466 nm, respectively, suggesting the generation of large aggregates in solution (Figure S41b). Moreover, a rod-like fiber was observed from the scanning electron microscopy (SEM) images, which directly supported the formation of high-molecular-weight linear supramolecular polymers (Figure S42).

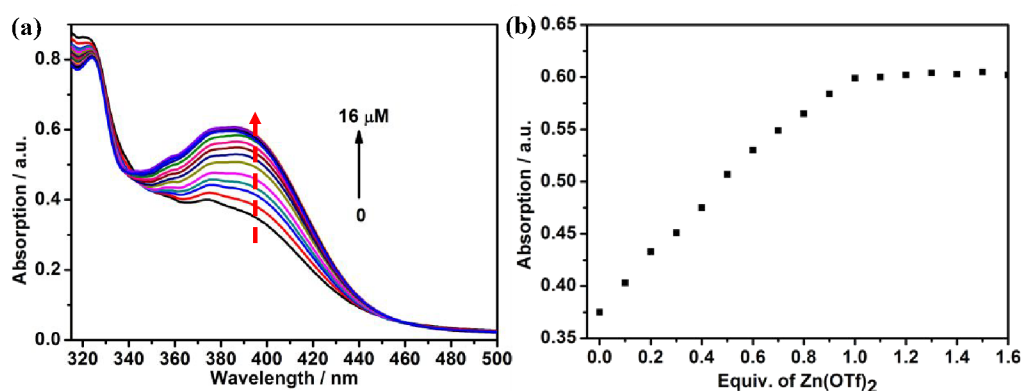


Figure 2. (a) Change in the absorption spectra upon stepwise addition of Zn(OTf)₂ to **3a** in CH₂Cl₂/CH₃CN (1/1, v/v); (b) Plot of the absorbance at 392 nm versus the amount of Zn(OTf)₂.

Furthermore, the B21C7 units within the linear supramolecular polymer provide another platform for incorporating the third non-covalent interaction, i.e., host-guest interaction, affording a cross-linked supramolecular polymer network. Firstly, the

1
2
3 complexation between crown ether and the secondary ammonium salt was selected as
4 a model system to study the binding strength during supramolecular polymerization
5 (Figure S43). The protons H_{4'} and H_{6'} on the bis-ammonium **5** downfield shifted,
6 while the signals of the protons on the crown ether of **2** upfield shifted. The
7 association constant between **2** and the mono-ammonium **7** (Figure S44) in
8 CD₃CN/CD₂Cl₂ determined by a ¹H NMR method was 4.6 (± 1.5) × 10² M⁻¹, which
9 indicated that the host-guest interaction suitable for the construction of the
10 cross-linked supramolecular assemblies (Figure S45 and S46).
11
12
13
14
15
16
17

18 The conversion from linear to cross-linked supramolecular polymers was then
19 accomplished by adding a bis-ammonium linker **5**. Concentration-dependent ¹H NMR
20 measurements were performed to investigate the formation of the cross-linked
21 supramolecular polymer as shown in Figure 3. A 1:1 mixture of **4a** and **5** was chosen
22 as the onset. With the increasing monomer concentration, noticeable chemical shift
23 changes for both precursors were observed. Upfield shifts were observed for the
24 signals of H₄ and H₅ of **4a**, whereas the H_{4'} and H_{6'} of the bis-ammonium linker **5**
25 shifted downfield. The peaks of all the proton signals became broader as the monomer
26 concentrations increased, suggesting the gradual formation of the cross-linked
27 supramolecular polymer. Furthermore, these observations also indicate that the Pt←N
28 coordination, the terpyridine-metal coordination and the host-guest interaction don't
29 interfere with each other in this system.
30
31
32
33
34
35
36
37
38
39
40
41
42
43
44
45
46
47
48
49
50
51
52
53
54
55
56
57
58
59
60

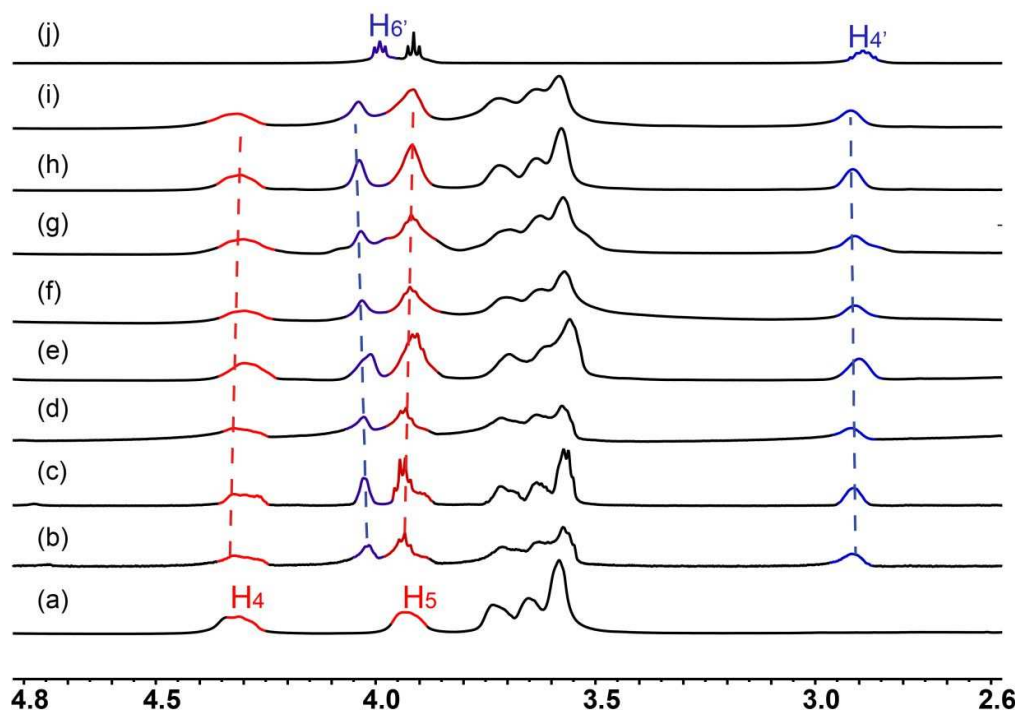


Figure 3. Partial ^1H NMR spectra ($\text{CD}_3\text{CN}/\text{CD}_2\text{Cl}_2$, 1/1, v/v, 295 K, 500 MHz) of (a) **4a**, (j) **5** and (b-i) **6a** (or 1:1 mixture of **4a** and **5**) at the concentration of B21C7 unit of (b) 1 mM (c) 5 mM (d) 10 mM (e) 20 mM (f) 30 mM (g) 40 mM (h) 50 mM (i) 60 mM.

Similarly, DOSY and DLS measurements were carried out to demonstrate the formation of the cross-linked supramolecular polymer **6a** in solution. From Figure 4a, as the concentration of B21C7/ammonium salt units in the supramolecular polymer increased from 5 to 60 mM, D decreased from 2.8×10^{-10} to $6.2 \times 10^{-11} \text{ m}^2 \text{ s}^{-1}$. From Figure 4b, as the concentration of B21C7/ammonium salt units increased from 2 to 60 mM, D_h increased from 109 to 715 nm, which were significantly larger than those of **4a** under the same concentrations of B21C7 units (Figure S47). These results demonstrate the formation of a cross-linked supramolecular polymer. Rheological experiments on the resulting gels were also conducted to study the viscoelastic properties (Figure 4c). The storage modulus (G') is always larger than the loss modulus (G'') and both are independent of the angular frequency ω , indicative of the formation of organogels. Additionally, the SEM image as shown in Figure 4d revealed an extended and interconnected fibrous network for the xerogel prepared by a freeze-drying method, giving direct evidence for the formation of the cross-linked

networks of **6a**.

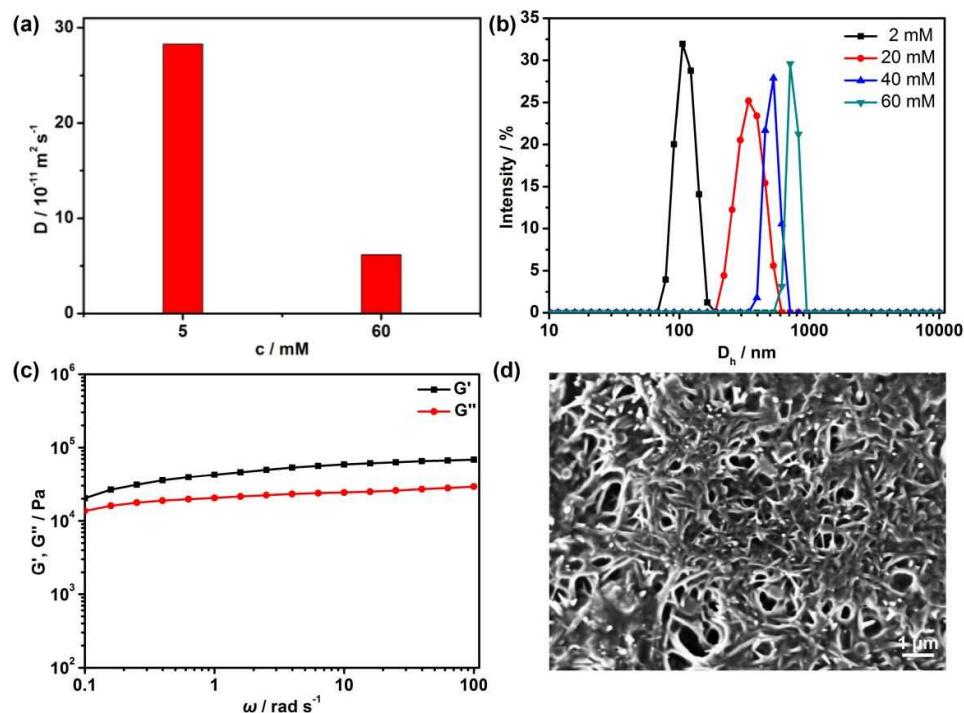


Figure 4. (a) Concentration dependence of diffusion coefficient D ($\text{CD}_3\text{CN}/\text{CD}_2\text{Cl}_2 = 1/1, v/v, 295$ K, 400 MHz) of **6a**; (b) Size distributions of **6a** at different concentrations of B21C7 units in the mixture of $\text{CH}_3\text{CN}/\text{CH}_2\text{Cl}_2$ (1/1, v/v); (c) G' and G'' versus ω for the gel with the concentration of B21C7 unit of 240 mM in $\text{CH}_3\text{CN}/\text{CH}_2\text{Cl}_2$ (1/1, v/v); (d) SEM image of **6a** with the concentration of B21C7 unit of 10 mM in $\text{CH}_3\text{CN}/\text{CH}_2\text{Cl}_2$ (1/1, v/v). The scale bar is 1 μm .

The supramolecular gel exhibited gel-sol transitions triggered by thermo, K^+ and 1,4,7,10-tetraazacyclododecane (cyclen) (Figure 5). Upon heating or the addition of K^+ , the gel turned into solution due to the destruction of the B21C7/secondary ammonium salt interactions. The addition of cyclen could weaken the coordination between Zn^{2+} and terpyridyl groups, accompanied with the degradation of the gel, which was evidenced by the titration UV-Vis absorption as shown in Figure S48. With the continuous addition of cyclen, the absorbance of the Zn^{2+} /terpyridyl band at 392 nm decreased. Adding 1.2 equiv. of cyclen resulted in the total disappearance of Zn^{2+} /terpyridyl absorption bands. After further addition of equal amounts of $\text{Zn}(\text{OTf})_2$, the absorption band at 392 nm reappeared. The gel could be reformed upon

further cooling or the addition of 18-crown-6 (18C6) or Zn^{2+} .

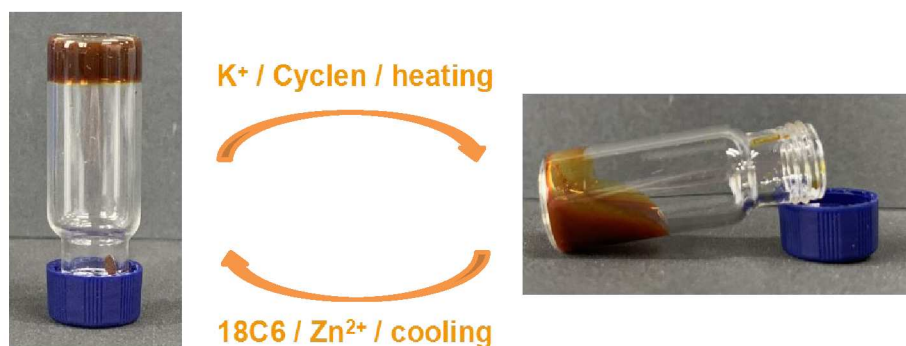


Figure 5. Optical photographs of the reversible gel-sol transition of the supramolecular network with the concentration of B21C7 unit of 240 mM in CH_3CN/CH_2Cl_2 (1/1, v/v).

The metallacycle-cored gel exhibits macroscopically self-healing properties which can be observed visually. From Figure 6, the crack on the gel with the length of 6 mm totally disappeared after 14 min. The self-healing process may be attributed to the dynamic and reversible metal coordination and host-guest interactions.

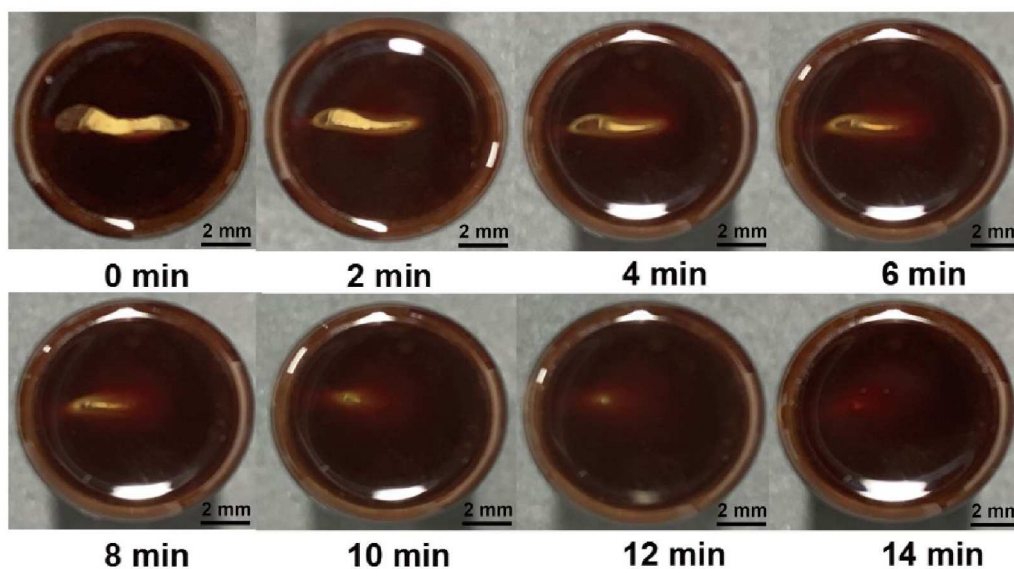
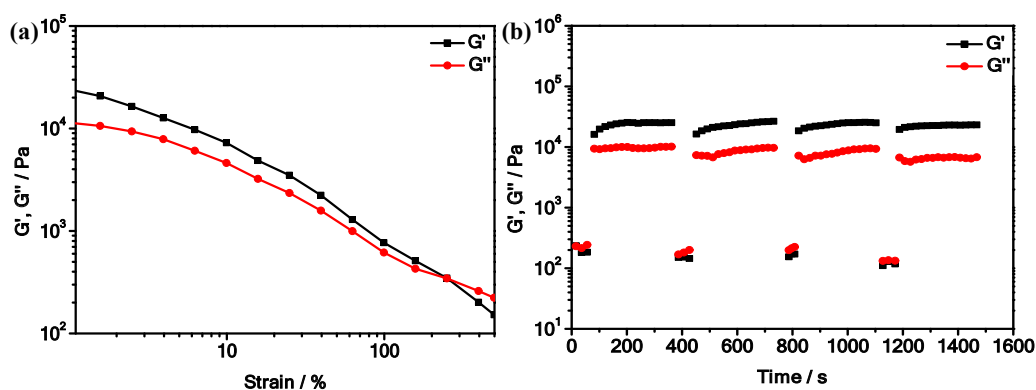


Figure 6. Photographs of the self-healing process of the supramolecular gel with the concentration of B21C7 unit of 240 mM in CH_3CN/CH_2Cl_2 (1/1, v/v). The gel was cut and left standing for 2 min, 4 min, 6 min, 8 min, 10 min, 12 min and 14 min, respectively.

Rheological tests were also performed to study the self-healing properties (Figure 7). The gels were subjected to strain sweep tests to obtain the broken strains. As the strain exceeded 240%, G' became smaller than G'' , suggesting that the gel was

1
2
3 destroyed (Figure 7a). Then the gel was studied under large (400%) and small (0.1%)
4 strains, respectively. As shown in Figure 7b, initially, when the strain was 400%, G''
5 was larger than G' , indicating that the gel was broken. Subsequently, the strain was
6 released to 0.1% and the gel was left standing for 60 s, and both G' and G'' returned
7 to their original values. This process could be repeated for four times without any loss of
8 the modulus. These observations indicate that the gel possesses good self-healing
9 properties.
10
11
12
13
14
15



16
17
18
19
20
21
22
23
24
25
26
27
28 **Figure 7.** (a) G' and G'' versus strain sweep. (b) Gel in continuous step-strain measurements. The
29 gel with the concentration of B21C7 unit of 240 mM in $\text{CH}_3\text{CN}/\text{CH}_2\text{Cl}_2$ (1/1, v/v) was subjected to
30 400% strain for 60 s, then back to 0.1% strain and retained for 60 s, in the linear regime for 300 s,
31 and four cycles were done.
32
33
34

35
36 The optical properties of the ligands, metallacycles, linear supramolecular
37 polymers and the cross-linked supramolecular polymers were studied by UV-Vis
38 absorption and fluorescence spectroscopy as shown in Figure 8 and Figure S49, and
39 the optical data are summarized in Table S1. From Figure 8, the absorption and
40 emission maxima of the metallacycles redshift with the increase of the
41 electron-donating ability of the substituents attached to the pyridyl ligands. Notably,
42 **3a** with amino substituents exhibits broad emission from 400 to 750 nm. The
43 fluorescence spectra maxima of the linear supramolecular polymers **4a** (539 nm) and
44 **4b** (473 nm) are largely redshifted relative to those of their corresponding
45 metallacycles **3a** (448 nm) and **3b** (430 nm), respectively, which can be attributed to
46 the extended conjugation arising from the zinc-terpyridine coordination. The
47 cross-linked supramolecular polymers exhibit emission wavelengths similar to those
48
49
50
51
52
53
54
55
56
57
58
59
60

of the linear supramolecular polymers. Moreover, as shown in Figure 8c and 8d, the emission spectra of **4a** and **6a** with amino substituents present more redshifts in comparison with those of **4b** and **6b** with hydrogen substituents. These results demonstrate that the optical properties could be effectively tuned via variation of the substituents of the precursor ligands.

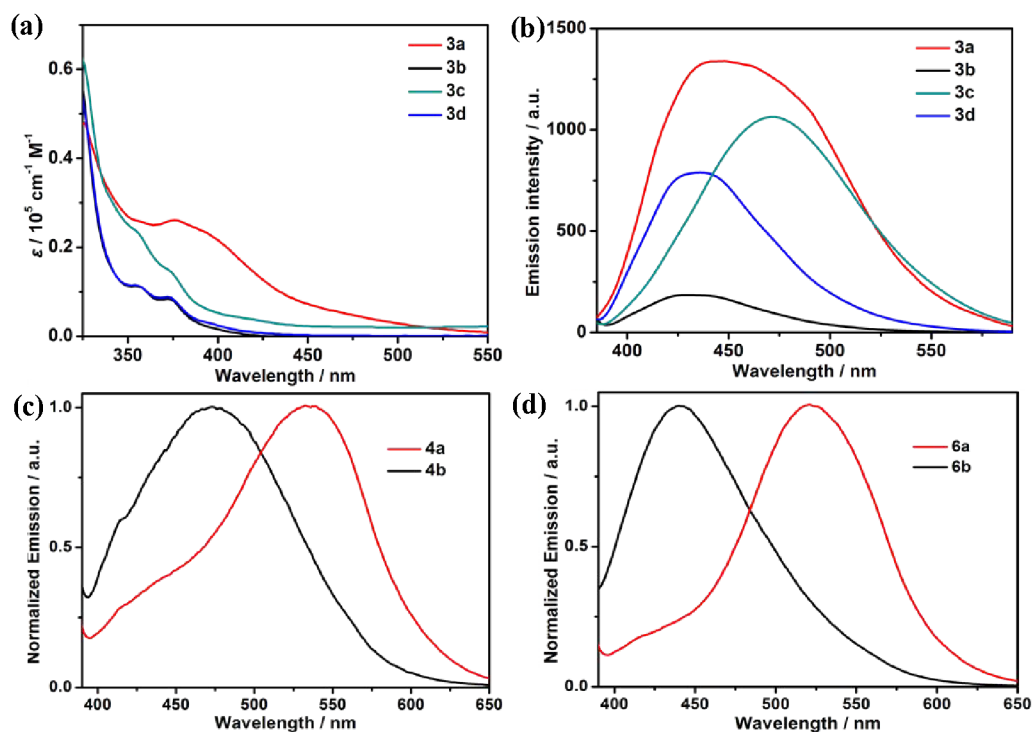


Figure 8. (a) Absorption and (b) emission spectra of metallacycles **3a-3d**. Normalized emission spectra of (c) **4a** and **4b**, and (d) **6a** and **6b**.

CONCLUSIONS

In conclusion, we have designed and constructed a new heterometallic bicyclic supramolecular polymer by means of orthogonal hierarchical self-assembly via platinum(II)-ligand coordination-driven self-assembly, zinc-terpyridine complex, and host-guest interactions. The gel obtained from high concentrations of this cross-linked supramolecular polymer exhibited dynamic properties, specifically thermo- and cation-induced sol-gel transitions. Via variation of the substituents on the precursor ligands, the optical properties of the supramolecular polymers could be effectively tuned. The combination of various metal-ligand coordination with orthogonal non-covalent interactions is a promising route to access novel

1
2
3 supramolecular polymers with interesting and useful characteristics.
4

5 ASSOCIATED CONTENT

6 Supporting Information

7
8
9 The Supporting Information is available free of charge on the ACS Publications
10 website at DOI:
11

12
13 Synthesis, NMR, ESI-TOF-MS, SEM, and UV-Vis data.
14
15

16 AUTHOR INFORMATION

17 Corresponding Authors

18
19
20 *yinsc@hznu.edu.cn

21
22 *stang@chem.utah.edu
23

24 Author Contributions

25
26 #Q.Z. and D.T. contributed equally to this work.
27
28

29 Notes

30
31 There are no conflicts to declare.
32

33 ACKNOWLEDGMENTS

34
35 S.Y. thanks National Natural Science Foundation of China (21971049 and 21574034)
36 and Zhejiang Provincial Natural Science Foundation of China (ZJNSF)
37 (LQ18B040001 and LY16B040006) for financial support. Q.Z. thanks National
38 Natural Science Foundation of China (51703046) and China Scholarship Council for
39 financial support. P.J.S. thanks NIH (Grant R01-CA215157) for financial support.
40
41
42
43
44

45 REFERENCES

- 46 (1) Cordier, P.; Tournilhac, F.; Soulié-Ziakovic, C.; Leibler, L. Self-Healing and Thermoreversible
47 Rubber from Supramolecular Assembly. *Nature* **2008**, *451*, 977.
48 (2) de Greef, T. F. A.; Meijer, E. W. Supramolecular Polymers. *Nature* **2008**, *453*, 171.
49 (3) Sangeetha, N. M.; Maitra, U. Supramolecular Gels: Functions and Uses. *Chem. Soc. Rev.* **2005**, *34*,
50 821.
51 (4) Sun, J. Y.; Zhao, X.; Illeperuma, W. R. K.; Chaudhuri, O.; Oh, K. H.; Mooney, D. J.; Vlassak, J. J.;
52 Suo, Z. Highly Stretchable and Tough Hydrogels. *Nature* **2012**, *489*, 133.
53 (5) Zhang, Y. S.; Khademhosseini, A. Advances in Engineering Hydrogels. *Science* **2017**, *356*, 3627.
54 (6) Kakuta, T.; Yamagishi, T.; Ogoshi, T. Stimuli-Responsive Supramolecular Assemblies Constructed
55
56
57

- 1
2
3 from Pillar[*n*]arenes. *Acc. Chem. Res.* **2018**, *51*, 1656.
- 4 (7) Burnworth, M.; Tang, L.; Kumpfer, J. R.; Duncan, A. J.; Beyer, F. L.; Fiore, G. L.; Rowan, S. J.;
5 Weder, C. Optically Healable Supramolecular Polymers. *Nature* **2011**, *472*, 334.
- 6 (8) Yang, Y.; Urban, M. W. Self-Healing Polymeric Materials. *Chem. Soc. Rev.* **2013**, *42*, 7446.
- 7 (9) Qin, B.; Zhang, S.; Song, Q.; Huang, Z.; Xu, J. F.; Zhang, X. Supramolecular Interfacial
8 Polymerization: A Controllable Method of Fabricating Supramolecular Polymeric Materials. *Angew.*
9 *Chem. Int. Edit.* **2017**, *56*, 7639.
- 10 (10) Stuart, M. A. C.; Huck, W. T. S.; Genzer, J.; Müller, M.; Ober, C.; Stamm, M.; Sukhorukov, G.
11 B.; Szleifer, I.; Tsukruk, V. V.; Urban, M.; Winnik, F.; Zauscher, S.; Luzinov, I.; Minko, S. Emerging
12 Applications of Stimuli-Responsive Polymer Materials. *Nat. Mater.* **2010**, *9*, 101.
- 13 (11) Yu, G. C.; Zhao, X. L.; Zhou, J.; Mao, Z. W.; Huang, X. L.; Wang, Z. T.; Hua, B.; Liu, Y. J.;
14 Zhang, F. W.; He, Z. M.; Jacobson, O.; Gao, C. Y.; Wang, W. L.; Yu, C. Y.; Zhu, X. Y.; Huang, F. H.;
15 Chen, X. Y. Supramolecular Polymer-Based Nanomedicine: High Therapeutic Performance and
16 Negligible Long-Term Immunotoxicity. *J. Am. Chem. Soc.* **2018**, *140*, 8005.
- 17 (12) Yan, X. Z.; Liu, Z. Y.; Zhang, Q. H.; Lopez, J.; Wang, H.; Wu, H. C.; Niu, S. M.; Yan, H. P.;
18 Wang, S. H.; Lei, T.; Li, J. H.; Qi, D. P.; Huang, P. G.; Huang, J. P.; Zhang, Y.; Wang, Y. Y.; Li, G. L.;
19 Tok, J. B. H.; Chen, X. D.; Bao, Z. N. Quadruple H-Bonding Cross-Linked Supramolecular Polymeric
20 Materials as Substrates for Stretchable, Antitearing, and Self-Healable Thin Film Electrodes. *J. Am.*
21 *Chem. Soc.* **2018**, *140*, 5280.
- 22 (13) Ma, C.; Lu, W.; Yang, X.; He, J.; Le, X.; Wang, L.; Zhang, J.; Serpe, M. J.; Huang, Y.; Chen, T.
23 Bioinspired Anisotropic Hydrogel Actuators with On - Off Switchable and Color - Tunable
24 Fluorescence Behaviors. *Adv. Funct. Mater.* **2018**, *28*, 1704568.
- 25 (14) Cui, Y. H.; Deng, R.; Li, Z.; Du, X. S.; Jia, Q.; Wang, X. H.; Wang, C. Y.; Meguellati, K.; Yang,
26 Y. W. Pillar[5]Arene Pseudo[1]Rotaxane-Based Redox-Responsive Supramolecular Vesicles for
27 Controlled Drug Release. *Mater. Chem. Front.* **2019**, *3*, 1427.
- 28 (15) Yin, Z.; Song, G.; Jiao, Y.; Zheng, P.; Xu, J. F.; Zhang, X. Dissipative Supramolecular
29 Polymerization Powered by Light. *CCS Chem.* **2019**, *1*, 335.
- 30 (16) Li, B.; He, T.; Fan, Y.; Yuan, X.; Qiu, H.; Yin, S. Recent Developments in the Construction of
31 Metallacycle/Metallacage-Cored Supramolecular Polymers via Hierarchical Self-Assembly. *Chem.*
32 *Commun.* **2019**, *55*, 8036.
- 33 (17) Li, B.; He, T.; Shen, X.; Tang, D.; Yin, S. Fluorescent Supramolecular Polymers with Aggregation
34 Induced Emission Properties. *Polym. Chem.* **2019**, *10*, 796.
- 35 (18) Yan, X. Z.; Wang, F.; Zheng, B.; Huang, F. H. Stimuli-Responsive Supramolecular Polymeric
36 Materials. *Chem. Soc. Rev.* **2012**, *41*, 6042.
- 37 (19) Beck, J. B.; Rowan, S. J. Multistimuli, Multiresponsive Metallo-Supramolecular Polymers. *J. Am.*
38 *Chem. Soc.* **2003**, *125*, 13922.
- 39 (20) Schmatloch, S.; Gonzalez, M. F.; Schubert, U. S. Metallo-Supramolecular Diethylene Glycol:
40 Water-Soluble Reversible Polymers. *Macromol. Rapid Commun.* **2002**, *23*, 957.
- 41 (21) Mei, J. F.; Jia, X. Y.; Lai, J. C.; Sun, Y.; Li, C. H.; Wu, J. H.; Cao, Y.; You, X. Z.; Bao, Z. N. A
42 Highly Stretchable and Autonomous Self-Healing Polymer Based on Combination of Pt \cdots Pt and π - π
43 Interactions. *Macromol. Rapid Commun.* **2016**, *37*, 1667.
- 44 (22) Schubert, U. S.; Eschbaumer, C. Macromolecules Containing Bipyridine and Terpyridine Metal
45 Complexes: Towards Metallosupramolecular Polymers. *Angew. Chem. Int. Edit.* **2002**, *41*, 2892.
- 46 (23) Housecroft, C. E. 4,2':6',4''-Terpyridines: Diverging and Diverse Building Blocks in Coordination
47
48
49
50
51
52
53
54
55
56
57
58
59
60

- 1
2
3 Polymers and Metallomacrocycles. *Dalton Trans.* **2014**, *43*, 6594.
- 4 (24) Gröger, G.; Meyer-Zaika, W.; Böttcher, C.; Gröhn, F.; Ruthard, C.; Schmuck, C. Switchable
5 Supramolecular Polymers from the Self-Assembly of a Small Monomer with Two Orthogonal Binding
6 Interactions. *J. Am. Chem. Soc.* **2011**, *133*, 8961.
- 7 (25) Lee, Y. H.; He, L. P.; Chan, Y. T. Stimuli-Responsive Supramolecular Gels Constructed by
8 Hierarchical Self-Assembly Based on Metal-Ligand Coordination and Host-Guest Recognition.
9 *Macromol. Rapid Commun.* **2018**, *39*, 6.
- 10 (26) Li, L. J.; Cong, Y.; He, L. P.; Wang, Y. Y.; Wang, J.; Zhang, F. M.; Bu, W. F. Multiple
11 Stimuli-Responsive Supramolecular Gels Constructed from Metal-Organic Cycles. *Polym. Chem.*
12 **2016**, *7*, 6288.
- 13 (27) Götz, S.; Abend, M.; Zechel, S.; Hager, M. D.; Schubert, U. S. Platinum-Terpyridine Complexes
14 in Polymers: A Novel Approach for the Synthesis of Self-Healing Metallopolymers. *J. Appl. Polym.*
15 *Sci.* **2019**, *136*, 47064.
- 16 (28) Zheng, Q.; Ma, Z.; Gong, S. Multi-Stimuli-Responsive Self-Healing Metallosupramolecular
17 Polymer Nanocomposites. *J. Mater. Chem. A*, **2016**, *4*, 3324.
- 18 (29) Cook, T. R.; Stang, P. J. Recent Developments in the Preparation and Chemistry of Metallacycles
19 and Metallacages via Coordination. *Chem. Rev.* **2015**, *115*, 7001.
- 20 (30) Fujita, M.; Tominaga, M.; Hori, A.; Therrien, B. Coordination Assemblies from a Pd(II)-Cornered
21 Square Complex. *Acc. Chem. Res.* **2005**, *38*, 369.
- 22 (31) Schmitt, F.; Freudenreich, J.; Barry, N. P. E.; Juillerat-Jeanneret, L.; Süß-Fink, G.; Therrien, B.
23 Organometallic Cages as Vehicles for Intracellular Release of Photosensitizers. *J. Am. Chem. Soc.*
24 **2012**, *134*, 754.
- 25 (32) Clever, G. H.; Punt, P. Cation–Anion Arrangement Patterns in Self-Assembled Pd₂L₄ and Pd₄L₈
26 Coordination Cages. *Acc. Chem. Res.* **2017**, *50*, 2233.
- 27 (33) Zhao, C.; Sun, Q.-F.; Hart-Cooper, W. M.; DiPasquale, A. G.; Toste, F. D.; Bergman, R. G.;
28 Raymond, K. N. Chiral Amide Directed Assembly of a Diastereo- and Enantiopure Supramolecular
29 Host and its Application to Enantioselective Catalysis of Neutral Substrates. *J. Am. Chem. Soc.* **2013**,
30 *135*, 18802.
- 31 (34) Mendez-Arroyo, J.; Barroso-Flores, J.; Lifschitz, A. M.; Sarjeant, A. A.; Stern, C. L.; Mirkin, C.
32 A. A Multi-State, Allosterically-Regulated Molecular Receptor With Switchable Selectivity. *J. Am.*
33 *Chem. Soc.* **2014**, *136*, 10340.
- 34 (35) Mosquera, J.; Ronson, T. K.; Nitschke, J. R. Subcomponent Flexibility Enables Conversion
35 between D₄-Symmetric Cd^{II}₈L₈ and T-Symmetric Cd^{II}₄L₄ Assemblies. *J. Am. Chem. Soc.* **2016**, *138*,
36 1812.
- 37 (36) Sanada, K.; Ube, H.; Shionoya, M. Rotational Control of a Dirhodium-Centered Supramolecular
38 Four-Gear System by Ligand Exchange. *J. Am. Chem. Soc.* **2016**, *138*, 2945.
- 39 (37) Zhang, Z.; Zhao, Z.; Hou, Y.; Wang, H.; Li, X.; He, G.; Zhang, M. Aqueous
40 Platinum(II)-Cage-Based Light-Harvesting System for Photocatalytic Cross-Coupling Hydrogen
41 Evolution Reaction. *Angew. Chem. Int. Edit.* **2019**, *58*, 8862.
- 42 (38) Kishi, N.; Akita, M.; Kamiya, M.; Hayashi, S.; Hsu, H.-F.; Yoshizawa, M. Facile Catch and
43 Release of Fullerenes Using a Photoresponsive Molecular Tube. *J. Am. Chem. Soc.* **2013**, *135*, 12976.
- 44 (39) Oliveri, C. G.; Gianneschi, N. C.; Nguyen, S. T.; Mirkin, C. A.; Stern, C. L.; Wawrzak, Z.; Pink,
45 M. Supramolecular Allosteric Cofacial Porphyrin Complexes. *J. Am. Chem. Soc.* **2006**, *128*, 16286.
- 46 (40) Xu, L.; Shen, X.; Zhou, Z.; He, T.; Zhang, J.; Qiu, H.; Saha, M. L.; Yin, S.; Stang, P. J.

1
2
3 Metallacycle-Cored Supramolecular Polymers: Fluorescence Tuning by Variation of Substituents. *J.*
4 *Am. Chem. Soc.* **2018**, *140*, 16920.

5 (41) Zhang, M.; Yin, S.; Zhang, J.; Zhou, Z.; Saha, M. L.; Lu, C.; Stang, P. J. Metallacycle-Cored
6 Supramolecular Assemblies with Tunable Fluorescence Including White-Light Emission. *Proc. Natl.*
7 *Acad. Sci. U. S. A.* **2017**, *114*, 3044.

8 (42) Zhang, M.; Saha, M. L.; Wang, M.; Zhou, Z.; Song, B.; Lu, C.; Yan, X.; Li, X.; Huang, F.; Yin,
9 S.; Stang, P. J. Multicomponent Platinum(II) Cages with Tunable Emission and Amino Acid Sensing.
10 *J. Am. Chem. Soc.* **2017**, *139*, 5067.

11 (43) Li, Z. Y.; Zhang, Y.; Zhang, C.-W.; Chen, L.-J.; Wang, C.; Tan, H.; Yu, Y.; Li, X.; Yang, H. B.
12 Cross-Linked Supramolecular Polymer Gels Constructed from Discrete Multi-pillar[5]arene
13 Metallacycles and Their Multiple Stimuli-Responsive Behavior. *J. Am. Chem. Soc.* **2014**, *136*, 8577.

14 (44) Shi, B.; Liu, Y.; Zhu, H.; Vanderlinden, R. T.; Shangguan, L.; Ni, R.; Acharyya, K.; Tang, J.-H.;
15 Zhou, Z.; Li, X.; Huang, F.; Stang, P. J. Spontaneous Formation of a Cross-Linked Supramolecular
16 Polymer Both in the Solid State and in Solution, Driven by Platinum(II) Metallacycle-Based Host-
17 Guest Interactions. *J. Am. Chem. Soc.* **2019**, *141*, 6494.

18 (45) Chen, L. J.; Yang, H. B. Construction of Stimuli-Responsive Functional Materials via Hierarchical
19 Self-Assembly Involving Coordination Interactions. *Acc. Chem. Res.* **2018**, *51*, 2699.

20 (46) Zheng, W.; Yang, G.; Shao, N. N.; Chen, L. J.; Ou, B.; Jiang, S. T.; Chen, G. S.; Yang, H. B. CO₂
21 Stimuli-Responsive, Injectable Block Copolymer Hydrogels Cross-Linked by Discrete
22 Organoplatinum(II) Metallacycles via Stepwise Post-Assembly Polymerization. *J. Am. Chem. Soc.*
23 **2017**, *139*, 13811.

24 (47) Hu, X.-Y.; Xiao, T.; Lin, C.; Huang, F.; Wang, L. Dynamic Supramolecular Complexes
25 Constructed by Orthogonal Self-Assembly. *Acc. Chem. Res.* **2014**, *47*, 2041.

26 (48) Yan, X.; Li, S.; Cook, T. R.; Ji, X.; Yao, Y.; Pollock, J. B.; Shi, Y.; Yu, G.; Li, J.; Huang, F.;
27 Stang, P. J. Hierarchical Self-Assembly: Well-Defined Supramolecular Nanostructures and
28 Metallohydrogels via Amphiphilic Discrete Organoplatinum(II) Metallacycles. *J. Am. Chem. Soc.*
29 **2013**, *135*, 14036.

30 (49) Yan, X.; Cook, T. R.; Pollock, J. B.; Wei, P.; Zhang, Y.; Yu, Y.; Huang, F.; Stang, P. J.
31 Responsive Supramolecular Polymer Metallogel Constructed by Orthogonal Coordination-Driven
32 Self-Assembly and Host/Guest Interactions. *J. Am. Chem. Soc.* **2014**, *136*, 4460.

33 (50) Lu, C.; Zhang, M.; Tang, D.; Yan, X.; Zhang, Z.; Zhou, Z.; Song, B.; Wang, H.; Li, X.; Yin, S.;
34 Sepehrpour, H.; Stang, P. J. Fluorescent Metallacycle-Core Supramolecular Polymer Gel Formed by
35 Orthogonal Metal Coordination and Host-Guest Interactions. *J. Am. Chem. Soc.* **2018**, *140*, 7674.

36 (51) Zhou, Z.; Yan, X.; Cook, T. R.; Saha, M. L.; Stang, P. J. Engineering Functionalization in a
37 Supramolecular Polymer: Hierarchical Self-Organization of Triply Orthogonal Non-covalent
38 Interactions on a Supramolecular Coordination Complex Platform. *J. Am. Chem. Soc.* **2016**, *138*, 806.

39 (52) Sepehrpour, H.; Saha, M. L.; Stang, P. J. Fe-Pt Twisted Heterometallic Bicyclic Supramolecules
40 via Multicomponent Self-Assembly. *J. Am. Chem. Soc.* **2017**, *139*, 2553.

For Table of Contents Only

